

## Frequency Dependence of $h/e$ Conductance Oscillations in Mesoscopic Ag Rings

John B. Pieper\* and John C. Price

*Department of Physics, Campus Box 390, University of Colorado, Boulder, Colorado 80309-0390*

(Received 19 July 1993)

We have measured the complex magnetoconductance of disordered mesoscopic Ag rings at frequencies from 250 Hz to 1.2 GHz. Conductance oscillations with flux period  $h/e$  are observed over the entire frequency range. No suppression of the  $h/e$  amplitude is seen up to our highest measurement frequency, even though it is several times the inverse sample transit time  $\tau_L^{-1}$ . An  $h/e$ -periodic imaginary part of the conductance is observed at frequencies  $\omega \gtrsim \tau_L^{-1}$ . The results suggest that the  $h/e$  oscillation would only be suppressed if  $\omega$  were greater than both  $\tau_L^{-1}$  and the thermal frequency  $kT/\hbar$ .

PACS numbers: 72.15.Gd, 71.55.Jv, 72.15.Rn

In the last ten years a rich variety of transport phenomena have been discovered in mesoscopic conductors [1]. In a mesoscopic system the sample dimensions are less than the dephasing length  $L_\phi$  and the electrons retain phase memory throughout the sample. Nearly all of the experiments and theoretical developments in this field have dealt with the zero-frequency conductance. A finite measurement frequency introduces a new time scale and may reveal qualitatively new effects, particularly if the new time scale is comparable with other characteristic times of the system, such as the carrier transit time. For samples in the diffusive limit the basic zero-frequency phenomena are the universal conductance fluctuations for simply connected samples and the Aharonov-Bohm conductance oscillations for multiply connected structures [2]. At finite frequency various nonlinear or mixing phenomena have been considered [3], but the more basic linear-response conductance and magnetoconductance at high frequencies have hitherto not been observed.

Extending the existing theoretical understanding of diffusive mesoscopic transport to finite frequencies is likely to be nontrivial. The dc conductance depends on the potentials at the contacts but not the detailed microscopic electric field within the conductor. This fact underlies the scattering matrix or Büttiker-Landauer theory of mesoscopic transport [4], and justifies the use of a spatially averaged perturbing electric field in treatments based on the Kubo formula [5]. By contrast, for the ac problem it may be necessary to include the detailed spatial dependence of the perturbing electric field [6]. There is a closely related concern that electron-electron interactions may play an important role in mesoscopics when the frequency is greater than the inverse transit time across the device [7]. These questions are fundamental to a full understanding of quantum transport, and illustrate the need for relevant experimental data.

We expect that the important frequency scales for a diffusive mesoscopic device are the inverse transit time  $\tau_L^{-1} = D/L^2$  and the thermal frequency  $kT/\hbar$ , where  $T$  is the device temperature,  $D$  is the electron diffusion constant, and  $L$  is the device size, taken to be one-half the circumference in the case of a ring. If the dephasing length is not much larger than the sample size then the

dephasing rate  $\tau_\phi^{-1} = D/L_\phi^2$  may also play a role. For samples made from disordered metal films these frequencies are typically in the rf and microwave region.

In this Letter we report measurements of the magnetoconductance of disordered Ag rings at frequencies  $\omega/2\pi$  from 250 Hz to 1.2 GHz. The rings have diameters  $d$  of 1.0 and 1.5  $\mu\text{m}$ , and the parameter  $\omega\tau_L$  varies from 0 to 2.2 for the smaller ring, and from 0 to 6.4 and 0 to 4.1 for the larger ones, over the frequency range used. However, the measurement frequencies are small compared to the temperature of 0.3 K. The parameter  $\hbar\omega/kT$  varies from 0 to 0.22 over our frequency range. The magnetoconductance data show oscillations of flux period  $h/e$  which persist to the highest measurement frequency used. The average magnitude of the oscillation amplitude of the real part of the conductance does not vary significantly from a constant from 0 to 1.2 GHz. An oscillatory imaginary part of the conductance is observed which has a constant average amplitude as a function of frequency for  $\omega\tau_L \geq 1$ .

The rings were patterned by electron-beam lithography on sapphire substrates using a single-layer PMMA resist. The 18–25 nm thick Ag films were thermally evaporated from a 99.999% pure source onto the substrates at a rate of 0.5 nm/s. The linewidths were approximately 80 nm. The rings were patterned with two leads of this same width, which connected to much larger wires at their ends. The length of each lead was chosen to be 0.5  $\mu\text{m}$  to give a total sample resistance near 50  $\Omega$ , providing a matched impedance for the ac measurement. Long Ag wires of the same width as the ring conductors were codeposited with the rings, and dc magnetoconductance measurements were made on the wires to extract the inelastic dephasing length  $L_\phi$ , and the spin-flip and spin-orbit scattering lengths  $L_s$  and  $L_{so}$ . The lengths were extracted by fitting the wire data by dc weak-localization theory including spin effects [8,9]. Spin scattering and dephasing lengths enter into mesoscopic effects in the singlet and triplet combinations  $L_0$  and  $L_1$ , where [10]

$$\begin{aligned} L_0^{-2} &\equiv L_\phi^{-2} + L_s^{-2}, \\ L_1^{-2} &\equiv L_\phi^{-2} + L_s^{-2} + \frac{4}{3} L_{so}^{-2}. \end{aligned} \quad (1)$$

TABLE I. Sample parameters.  $d$  is the ring diameter.  $L_0$  and  $L_1$  are the singlet and triplet diffusion lengths, determined by measurements of the weak-localization magnetoconductance of long wires codeposited with the rings.  $D$  is an estimate of the diffusion constant obtained from the dc resistance of the rings, and  $\tau_L$  is the diffusive transit time across the ring, equal to  $(\pi d/2)^2/D$ . Uncertainties in  $L_0$  and  $L_1$  are 1 in the last digit.

Sample	$d$ ( $\mu\text{m}$ )	$L_0$ ( $\mu\text{m}$ )	$L_1$ ( $\mu\text{m}$ )	$D$ ( $\text{cm}^2/\text{s}$ )	$\tau_L$ (ns)
1	1.0	2.4	0.39	85	0.29
2	1.5	2.2	0.50	65	0.85
3	1.5	1.6	0.41	104	0.54

The diffusion constant  $D$  was estimated using  $D = \frac{1}{3} v_F l$ , taking the free-electron value for the Fermi velocity ( $1.39 \times 10^6$  m/s for Ag) and estimating the mean free path  $l$  from the sample dimensions and the measured dc resistance. We have shown in previous experiments on the frequency dependence of weak localization in wires that the diffusion constant can be estimated accurately in this way [11]. The parameter  $k_F l$  describing the degree of disorder was estimated to be  $\approx 200$  for these rings. The parameters characterizing the samples are given in Table I.

All measurements were made at temperatures from 0.30 to 0.35 K in a  $^3\text{He}$  evaporation cryostat. The dc measurements were made using a conventional low-frequency bridge operated near 250 Hz. The high-frequency measurements were made with a homodyne reflectometer designed for the range 0.2–1.2 GHz. The sample was connected to the reflectometer through a semirigid coaxial line, for which the sample served as a lumped-element termination. The output of the reflectometer measured the complex reflection coefficient of the nominally 50  $\Omega$  sample. Small changes in the reflection coefficient are closely proportional to changes in the complex conductance. The reflectometer was calibrated for each measurement with the sample in place by comparing its output with measurements of the dc resistance, as the sample temperature was varied from 10 to 30 K. At these temperatures the quantum effects are suppressed, and the conductance change is due to changes of the Drude relaxation time. The variation of conductance with temperature is therefore to high accuracy purely real and independent of frequency, up to frequencies of order the inverse Drude time ( $\approx 10^{13}$  Hz for our samples). This calibration directly determines both the magnitude and phase of the complex magnetoconductance, eliminating the need for measurements of the electrical length of the transmission line or any other phase shifts in the system. A description of the circuit and further details of its operation have been given elsewhere [12], and our method has been demonstrated in previous experiments on weak localization [11].

In the experiments reported here the final connections to the sample chip were made by Al wire bonds. All measurements were made with a magnetic field larger

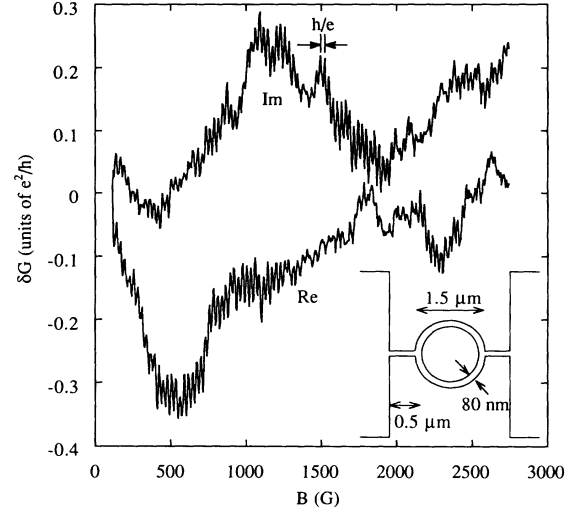


FIG. 1. The complex magnetoconductance of a 1.5  $\mu\text{m}$  diam Ag ring (sample 2) at 1.03 GHz, with the field perpendicular to the plane of the ring. The conductance at the lowest field strength (114 G) has been subtracted. The data were recorded at 0.35 K with a dissipated power of 50 pW. A drawing of the ring with dimensions is included.

than the critical field of Al ( $\approx 100$  G) so that there was no background magnetoconductance due to the presence of a superconductor. The total power dissipated in the ring and narrow leads was 50 pW in all measurements. Tests were performed with varying excitation currents to determine whether electrons in the sample were being heated significantly above the substrate temperature. The  $h/e$  amplitude increased linearly with the current  $I$  for dissipated powers up to 70 pW, indicating no significant electron heating. At higher currents the data suggested an  $I^{1/2}$  increase, which may be attributable to energy averaging due to the potential difference across the ring [13]. In addition, a test in which the substrate temperature was varied over the range 0.35–1.0 K clearly showed temperature dependence of the  $h/e$  amplitude, indicating that the electron temperature was not saturated at some higher value. These tests were conducted both at dc and at 720 MHz, with similar results. Repeated conductance traces taken with time delays of an hour or less were highly reproducible.

A sample of the ac magnetoconductance data is shown in Fig. 1. The amplitude of the oscillations in the real part shown here is typical of that found at all frequencies including dc, and is rather small compared to the “universal” value  $e^2/h$ . The amplitude at dc can be explained as follows. First, the contribution of the spin triplet to the oscillation should be strongly suppressed due to the strong spin-orbit effect in Ag which gives a triplet length  $L_1 \ll L$ . The contribution of the singlet is limited to a lesser degree by the length  $L_0$ , which is dominated by the spin-flip scattering length and is comparable to the size of the ring (see Table I). The presence of leads connecting the ring to the measuring apparatus is known to reduce

the oscillation amplitude [14]. Finally, at finite temperature the oscillations are suppressed by a factor [15]  $(E_c/kT)^{1/2}$ , where  $E_c$  is the correlation energy  $\pi^2\hbar D/L^2$ . By neglecting the triplet term, using for the singlet term a calculation by Fal'ko [16] which includes spin-flip scattering and the effect of leads, and taking into account the energy averaging at our measurement temperature, we calculate an expected value for the dc amplitude which agrees with the measured values to within a factor of 2.

The rms  $h/e$  amplitudes in the rings are plotted against frequency in Fig. 2. In order to obtain an ensemble average and a measure of the dispersion, all the magnetoconductance data were broken into sets of length approximately equal to the correlation field  $B_c$ , which was estimated by examining field autocorrelations of the data. The amplitude in each set is thus, according to the ergodic hypothesis [17], roughly equivalent to the amplitude in a different ensemble member. The Fourier power spectrum of each set was calculated and the value of the mean squared amplitude was found by integrating over a fixed range around the peak at  $h/e$ . The distributions of amplitudes found in this way were used to determine the mean amplitudes with the accuracy shown by the error bars in Fig. 2. The frequency where  $\omega\tau_L=1$  is indicated for each sample by the vertical dashed line. The averaged amplitude of the real part is seen to be essentially constant from dc to 1.2 GHz in both 1.0 and 1.5  $\mu\text{m}$  diam rings. The imaginary part is also essentially constant from 0.5 to 1.2 GHz. The phase calibration of the reflectometer in the complex conductance plane is reproducible to within a few degrees. Errors of this size are not sufficient to explain the measured imaginary part.

One might expect from a time-domain picture of quantum interference that a frequency larger than  $\tau_L^{-1}$  would suppress conductance oscillations. The probability density for an electron to arrive at a net displacement  $L$  at time  $t$  by diffusion is proportional to  $t^{-1/2}\exp(-L^2/4Dt)$  in quasi one dimension; i.e., it is peaked at times of order  $\tau_L$ . In the frequency domain one could expect this to lead to a cutoff for  $\omega\tau_L > 1$ . Indeed, in the theory of weak localization [18,19], the amplitude of the  $h/2e$  oscillations in a ring is suppressed as  $[L_\varphi(\omega)/L]\exp[-2L/L_\varphi(\omega)]$ , where  $L_\varphi(\omega) \equiv (L_\varphi^{-2} - i\omega/D)^{-1/2}$ , giving just such a cutoff. (We assume the weak-field limit for the ac measurement field, so that time-reversal symmetry is broken only by the magnetic field.) At dc the mean squared amplitude of the  $h/e$ -period oscillation is suppressed by dephasing [20] as  $(L_\varphi/L)\exp(-2L/L_\varphi)$  when  $L > L_\varphi$ . Using the substitution  $L_\varphi \rightarrow (L_\varphi^{-2} - i\omega/D)^{-1/2}$  which occurs in weak-localization theory would then result in an exponential cutoff for the  $h/e$  oscillations as well. In the case of weak localization this combination of the frequency and dephasing rate has been verified by recent experiments in both quasi one [11] and quasi two [21] dimensions. Our data in Fig. 2 clearly do not show this ex-

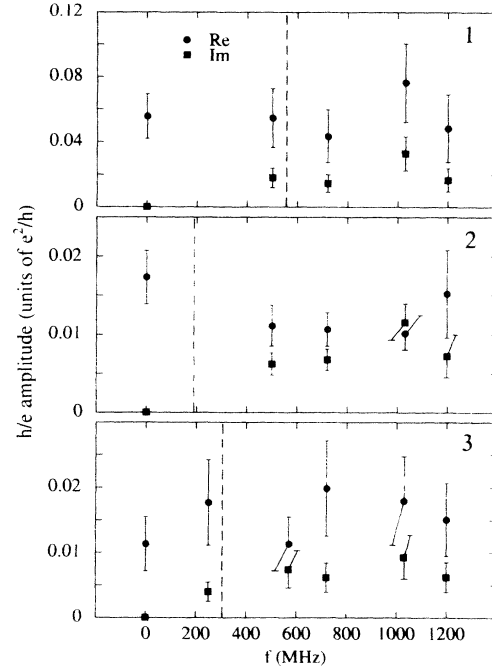


FIG. 2. The rms amplitudes of  $h/e$ -period magnetoconductance oscillations in Ag rings (samples 1, 2, and 3) at frequencies from near dc to 1.2 GHz. The results shown here were extracted from about 500 h total measurement time. The measurements were made at 0.3–0.35 K with an average dissipated power of 50 pW. The error bars give the uncertainty ranges for the mean amplitudes at the 90% confidence level. The size of the error bars is a consequence of the finite number of field correlation lengths in the data. The vertical dashed lines mark frequencies where  $\omega\tau_L=1$ .

ponential suppression with frequency for frequencies above  $\tau_L^{-1}$ .

We may also compare the data with the simplest possible extension of the dc theory to high frequencies. We have evaluated the simplest conductance correlation diagram for noninteracting electrons using the impurity diagram technique, at nonzero frequency and at finite temperature [22]. The calculation predicts a nearly frequency-independent real part of the conductance oscillations (for  $\omega < kT/\hbar$ ) and an imaginary part which is frequency independent in the range  $\tau_L^{-1} < \omega < kT/\hbar$ . However, the theory is not in quantitative agreement with the data. In particular, it predicts a real to imaginary amplitude ratio near unity for  $\tau_L^{-1} < \omega < kT/\hbar$ , which does not seem to be consistent with the data in Fig. 2.

We note that a frequency-independent real amplitude for the ensemble average, together with a frequency-dependent imaginary amplitude for the ensemble average, is not a violation of the Kramers-Kronig relations. Instead, the appearance of the imaginary part implies that, for a particular sample at fixed flux, the real part of the  $h/e$  component of the conductance fluctuates as a function of frequency. Since the imaginary part is present at

frequencies comparable to the inverse transit time  $\tau_L^{-1}$ , the data suggest that the two-frequency correlation function  $\langle \text{Re}[\delta G(\omega, B)] \text{Re}[\delta G(\omega', B')] \rangle$  decays when  $|\omega - \omega'| > \tau_L^{-1}$ .

We have observed  $h/e$ -periodic conductance oscillations at frequencies which exceed the inverse diffusive transit time by up to a factor of 6. Although the transit time is the characteristic time for diffusive paths which encircle the ring, there is no large change in the ensemble-averaged real part of the amplitude at these frequencies. An imaginary part of the oscillation amplitude is observed at frequencies of order the inverse transit time, indicating that the conductance oscillations for a given sample fluctuate as a function of frequency.

We thank G. Zimmerli and J. Martinis for advice on fabrication, and S. Feng and F. Von Oppen for helpful discussions. This work was supported by the Office of Naval Research under Grant No. N00014-90-J-1891, by the National Science Foundation under Grant No. DMR-9057426, and by the David and Lucile Packard Foundation.

---

\*Present address: Department of Applied Physics, Yale University, P.O. Box 208284, New Haven, CT 06520.

- [1] For reviews see *Mesoscopic Phenomena in Solids*, edited by B. L. Altshuler, P. A. Lee, and R. A. Webb (North-Holland, Amsterdam, 1991).
- [2] See Ref. [1] and A. G. Aronov and Yu. V. Sharvin, *Rev. Mod. Phys.* **59**, 755 (1987); S. Washburn and R. A. Webb, *Adv. Phys.* **35**, 422 (1986); Y. Imry, in *Directions in Condensed Matter Physics*, edited by G. Grinstein and G. Mazenko (World Scientific, Singapore, 1986), Vol. 1; Shechao Feng and Patrick A. Lee, *Science* **251**, 633 (1991).
- [3] V. Fal'ko, *Europhys. Lett.* **8**, 785 (1989); V. I. Fal'ko and D. E. Khmel'nitskii, *Zh. Eksp. Teor. Fiz.* **95**, 328 (1989) [*Sov. Phys. JETP* **68**, 186 (1989)]; A. G. Aronov and V. E. Kravtsov (to be published); J. J. Lin, R. E. Bartolo, and N. Giordano, *Phys. Rev. B* **45**, 14231 (1991).
- [4] M. Büttiker, *Phys. Rev. Lett.* **57**, 1761 (1986).
- [5] C. L. Kane, R. A. Serota, and P. A. Lee, *Phys. Rev. B* **37**, 6701 (1988).
- [6] M. Büttiker, A. Prêtre, and H. Thomas, *Phys. Rev. Lett.* **70**, 4114 (1993); R. Landauer, *Phys. Scr.* **T42**, 110 (1992).
- [7] Y. B. Levinson and B. Shapiro, *Phys. Rev. B* **46**, 15520 (1992).
- [8] S. Hikami, A. I. Larkin, and Y. Nagaoka, *Prog. Theor. Phys.* **63**, 707 (1980).
- [9] B. L. Al'tshuler and A. G. Aronov, *Pis'ma Zh. Eksp. Teor. Fiz.* **33**, 515 (1981) [*JETP Lett.* **33**, 499 (1981)].
- [10] V. Chandrasekhar, P. Santhanam, and D. E. Prober, *Phys. Rev. B* **42**, 6823 (1990).
- [11] John B. Pieper, John C. Price, and John M. Martinis, *Phys. Rev. B* **45**, 3857 (1992).
- [12] John B. Pieper and John C. Price, *Rev. Sci. Instrum.* **65**, 445 (1994).
- [13] A. I. Larkin and D. E. Khmel'nitskii, *Zh. Eksp. Teor. Fiz.* **91**, 1815 (1986) [*Sov. Phys. JETP* **64**, 1075 (1986)].
- [14] Y. Isawa, H. Ebisawa, and S. Maekawa, *J. Phys. Soc. Jpn.* **55**, 2523 (1986); V. Chandrasekhar, P. Santhanam, and D. E. Prober, *Phys. Rev. B* **44**, 11203 (1991).
- [15] P. A. Lee, A. D. Stone, and H. Fukuyama, *Phys. Rev. B* **35**, 1039 (1987).
- [16] V. I. Fal'ko, *J. Phys. Condens. Matter* **4**, 3943 (1992).
- [17] P. A. Lee and A. D. Stone, *Phys. Rev. Lett.* **55**, 1622 (1985).
- [18] L. P. Gor'kov, A. I. Larkin, and D. E. Khmel'nitskii, *Pis'ma Zh. Eksp. Teor. Fiz.* **30**, 248 (1979) [*JETP Lett.* **30**, 228 (1979)].
- [19] B. L. Al'tshuler, A. G. Aronov, and B. Z. Spivak, *Pis'ma Zh. Eksp. Teor. Fiz.* **33**, 101 (1981) [*JETP Lett.* **33**, 94 (1981)].
- [20] Aronov and Sharvin, Ref. [2].
- [21] G. U. Sumanasekera, B. D. Williams, D. V. Baxter, and J. P. Carini, *Solid State Commun.* **85**, 941 (1993).
- [22] The diagram we have evaluated is Fig. 5(a) of Lee, Stone, and Fukuyama, Ref. [15]. See also John B. Pieper and John C. Price, *Phys. Rev. B* (to be published).